Tomographic Assessment of Cerebral Perfusion Using a Single-Photon Emitter (Krypton-81m) and a Rotating Gamma Camera

F. Fazio, C. Fieschi, M. Collice, M. Nardini, F. Banfi, M. Possa, and F. Spinelli

Ospedale Niguarda, Milan, Department of Neurology, Rome, Italy, and Hammersmith Hospital, London, U.K.

Continuous carotid infusion of short-lived krypton-81m ($t_{1/2}$ 13 sec) yields an assessment of regional cerebral perfusion. This assessment can be obtained in three dimensions if activity is recorded with a rotating gamma camera and a computer to reconstruct krypton-81m distribution in tomographic sections. These showed several advantages over conventional views: (a) visualization of blood-flow distribution within brain structures (gray and white matter, basal ganglia); (b) more accurate location and evaluation of areas of relatively reduced or increased perfusion; (c) better definition of patterns of collateral circulation; (d) greater sensitivity and specificity in detecting and defining blood-flow changes during physiological activation studies. A limitation of the krypton-81m technique is its invasiveness. However, this study shows that the combination of new advances in radiochemistry with single-photon emission computed tomography may result in accessible methods for assessing, noninvasively and in three dimensions, the behavior of cerebral function in man.

J Nucl Med 21: 1139–1145, 1980

A major limitation in the capability of assessing the distribution of radioactivity in a living object is that the present generation of nuclear medicine imaging systems yields two-dimensional images of three-dimensional objects. Even when an excellent resolution in the frontal plane is achieved (as with modern gamma cameras), the resolution in depth will inevitably be very poor, depending essentially on the thickness of the organ studied. This error is commonly minimized by taking multiple views, thus leaving to the interpreter's brain the reconstruction of a grossly three-dimensional image of the object.

This problem becomes of crucial relevance in complex organs, such as the heart or the brain. In these organs it is impossible, even from multiple views, to obtain "clean" information on different structures within the organ itself, without interference from adjacent regions.

Received Feb. 19, 1980; revision accepted July 8, 1980.

For reprints contact: F. Fazio, MD, Servizio di Medicina Nucleare, Ospedale S. Raffaele, Via Olgettina 60, 20090 Milano-Segrate, Italy.

The prevention of superimposition of information with depth in nuclear medicine is the purpose of computer-assisted tomography (*1*). This can generally be divided into two categories: PCT using the annihilation radiation from positron emitters, and ECT for "single-photon" emitters. Each approach has advantages and disadvantages (*1*). From the technical standpoint, systems based on positron emission are more accurate, since constant resolution and more-uniform sensitivity with depth can be achieved by the electronic collimation of coincidence counting. Furthermore, three of the most important biological elements (C, O, and N) provide positron emitters (C-11, O-15, and N-13) but no useful single-gamma emitters. Positron emission tomography is now being actively exploited for the noninvasive, three-dimensional assessment of blood flow and metabolism in the brain. Unfortunately, due to the complexity and high cost of the equipment required (a dedicated cyclotron and a single-purpose tomograph), this approach is restricted to a few privileged centers. It would be of interest if an accurate assessment of regional cerebral function could be available on a much broader basis. This could be

achieved by single-photon ECT, which yields the tomographic distribution in vivo of commercially available tracers, such as Tc-99m I-123, Kr-81m, etc. ECT can be obtained using either a specially designed tomograph (*2–4*) or an Anger gamma camera equipped with a rotating gantry (*5–7*).

The purpose of this paper is to show the feasibility of obtaining tomographic images of brain perfusion using continuous carotid infusion of Kr-81m and a rotating gamma camera.

METHODS

Continuous carotid infusion of Kr-81m in solution, used in conjunction with an ordinary Anger camera, provides images of cerebral perfusion in two dimensions (*8*). Krypton-81m is a 13-sec radionuclide that can be produced continuously (either as a gas or in solution) in a generator from its parent, Rb-81 ($T_{1/2}$ = 4.6 hr). Krypton-81m emits photons carrying 190 keV, which is an ideal energy for recording with a gamma camera. Due to its short half-life, continuous carotid infusion of Kr-81m in solution will never result in the equilibration of this diffusible tracer within the brain; continuous recording of the activity over the brain during the infusion will therefore reflect, at any time, regional *arrival* of the tracer—namely regional perfusion (*8*). Other longer-lived radioactive gases (Xe-133, Xe-127, Kr-85, Kr-77, N-13), when continuously infused, will eventually equilibrate within the brain, thus measuring cerebral volume rather than flow. The very short half-life of Kr-81m permits the assessment of cerebral perfusion under steady-state conditions, thus providing the very high counting rates required for ECT (*1*).

The Rb-81 → Kr-81m generator was produced in England on the MRC Cyclotron and shipped to Milan by commercial flights, being available all day after a morning production. Krypton-81m can be recovered continuously from its generator in the solution phase by passing 5% dextrose through a cation-exchange column, which binds the parent Rb-81 (*9,10*). The Kr-81m was continuously infused into the internal carotid artery of patients with various cerebrovascular disorders following routine contrast angiography. During the infusion, the radioactivity over the head was recorded by means of a commercial device designed for single-photon computerized tomography.* This consists of a conventional large-field gamma-camera detector equipped with parallel-hole collimators and mounted on a rotating mechanical gantry. This allows a 360° rotation of the detector around the long axis of the patient at a constant, adjustable speed (2–20 min/rotation). The diameter of rotation can be selected from 18 to 54 cm. The camera is also suitable for whole-body emission tomography and for conventional two-dimensional static and dynamic imaging. During the detector's rotation, data were sampled every 5° 36′ (64 views) and recorded using a 64 × 64 matrix on a computer with a 32K/16-bit memory.†

The arithmetic means of opposite views were then computed in order to compensate for loss of resolution with depth (*11*). Tomographic sections were then reconstructed using a filtered back-projection reconstruction algorithm with a modifiable filter (*12*). At the time of reconstruction, data were also corrected for attenuation by assuming uniform absorption within the head and using an inversion formula that involves modifying the Fourier transform of the projection data in such a way that the modification represents the Fourier transforms of unattenuated data. The algorithm is described in detail in Ref. *13* and is summarized in the Appendix. A complete set of tomographic slices effectively constitutes a three-dimensional reconstruction of the whole activity in the field of view. This can then be displayed as a series of horizontal, or coronal, or even oblique slices. Theoretically, 64 such sections could be obtained, the thickness of each section corresponding to the width of each pixel, which is 6.8 × 6.8 mm (5.5 × 5.5 in the expanded mode). In practice, however, there is a limiting factor due to the spatial resolution of the reconstructed slice. This was calculated, for the system, using line sources inserted into holes drilled at different depths in a Plexiglas phantom. Results were essentially identical to those obtained by Murphy et al. (*7*), yielding an average resolution of 1.6 cm FWHM and, after attenuation correction, relative constancy of spatial resolution across the field of view. Thus the minimum slice thickness is 1.6 cm FWHM (using a single pixel plane). Using a plane made by summing two or more adjacent pixels, however, the respective slice thickness would not increase proportionally. It can be shown that for the expanded mode (5.5- by 5.5-mm pixel size) the actual slice thickness would be 1.8 cm FWHM for a two-pixel plane and 2.0 cm FWHM for a three-pixel plane (M. Myers, personal communication).

Both the horizontal and coronal slices that will be shown in this paper are obtained by summing the activity of two adjacent pixels; the effective thickness of these slices will thus be 1.8 cm FWHM. There is considerable overlap, therefore, between adjacent slices; at FWTM there is still more overlap.

For each run approximately 3 million counts were collected; this was achieved in 2–8 min, according to the activity of the generator. This corresponds to an absorbed radiation dose to the brain (target organ) of less than 50 mrad. Each run yielded a set of eight to ten horizontal and a set of 14–16 coronal sections spaced 1.1 cm center to center. However, as pointed out before, there is an overlap between sections, the effective thickness of each section being of the order of 2 cm.

In this paper, coronal and horizontal sections will be conventionally labeled with progressive numbers starting, respectively, from the front and the base of the skull.

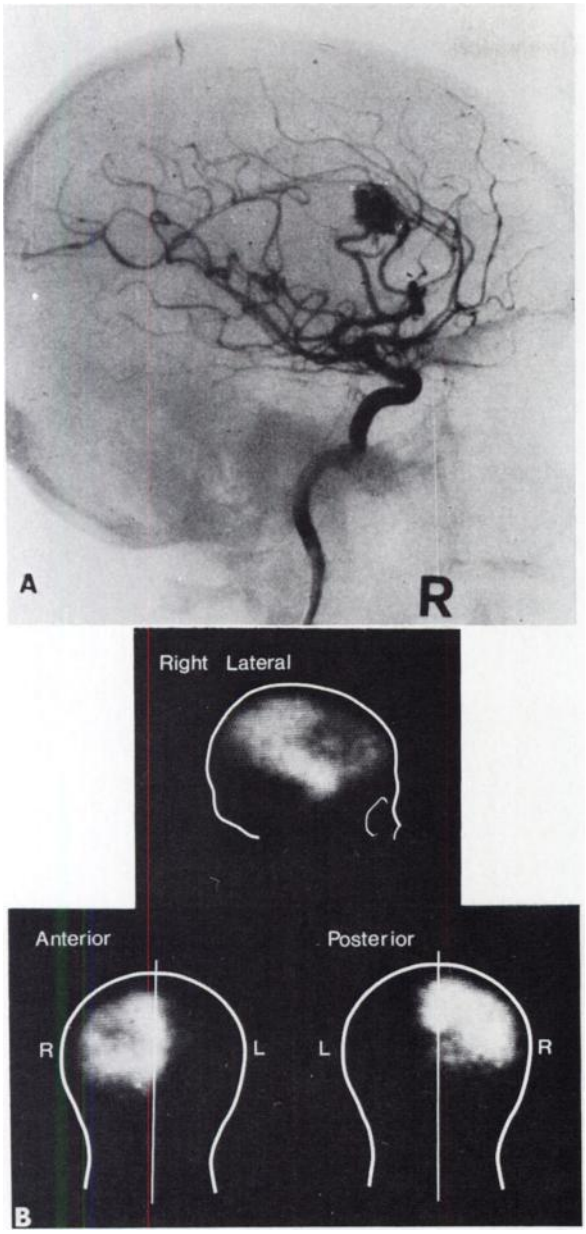

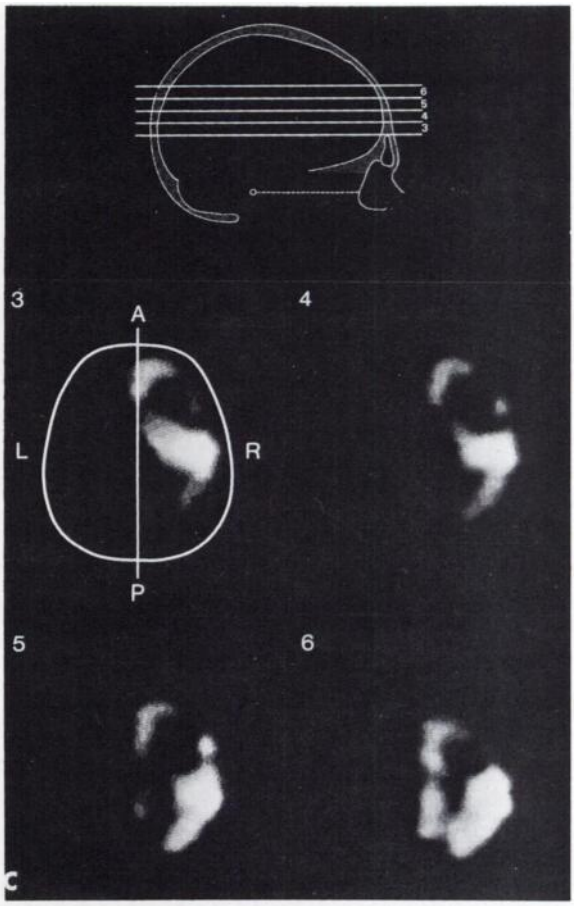

FIG. 1. Right fronto-lateral arteriovenous malformation. (A) Right carotid angiogram. (B) conventional two-dimensional Kr-81m perfusion images of right hemisphere. (C) perfusion in reconstructed horizontal tomographic sections. Section thickness 1.1 cm center to center.

The first horizontal section passes 3 cm above the auditory meatus and is parallel to the orbito-meatal line; the first coronal section passes across the frontal region, ~3 cm beyond the external layer of the frontal bone (glabella), on a plane perpendicular to the orbito-meatal line.

RESULTS

The tomographic assessment of cerebral perfusion was obtained in nine patients with various brain diseases. Diagnoses were established on clinical and angiographic grounds, aided by transmission computerized tomography. In all the cases studied, ECT reconstructions, unlike conventional Kr-81m two-dimensional images, provided assessment of the relative blood flow in different brain structures (gray and white matter, basal ganglia). In patients with space-occupying lesions or cerebrovascular disease, they also provided more accurate location and evaluation of perfusion alterations. In four patients with complete occlusion of one internal carotid artery, ECT also allowed better definition and evaluation of collateral circulation patterns. In addition, tomographic reconstructions showed greater accuracy, relative to conventional views, in describing blood-flow changes during physiological studies. Two clinical examples and the results of a left hemisphere activation study will be shown in detail.

Case 1. A patient presented with signs of moderate intracranial hypertension and slight left hemiparesis. Right carotid angiogram (Fig. 1A) showed a frontolateral arteriovenous malformation (AVM) as well as indirect signs of a space-occupying lesion. Transmission CT scan revealed a high-density lesion in the frontolateral region. Krypton-81m conventional two-dimensional views (Fig. 1B) showed an area of reduced perfusion in the frontal lobe. In the right lateral view, a denser spot sitting in the middle of the cold area was noted, a firm interpretation of this finding not being possible on the

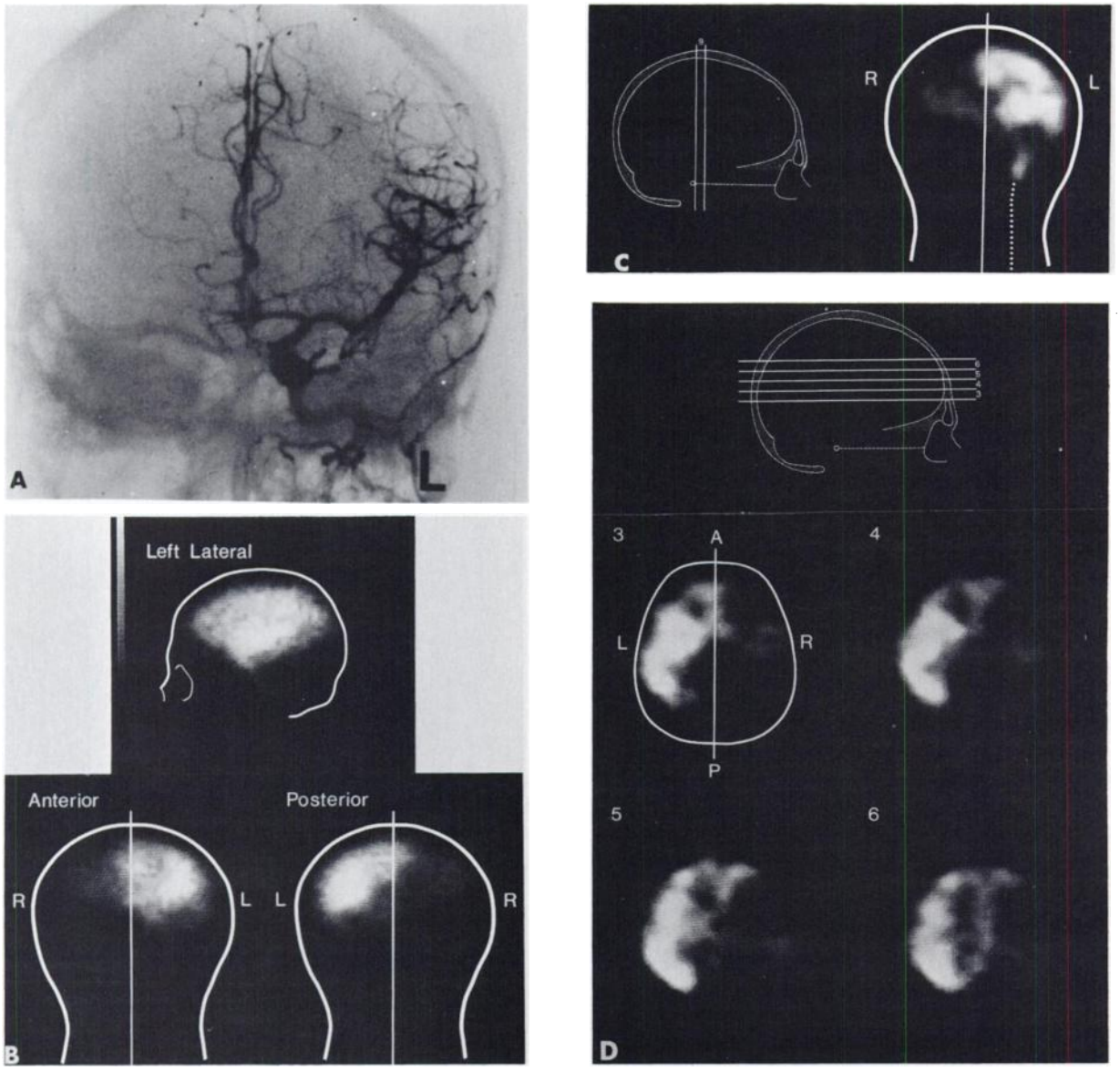

FIG. 2. Occlusion of right internal carotid artery. (A) left carotid angiogram. (B) conventional Kr-81m two dimensional projections (infusion in left carotid artery). (C) perfusion in a coronal tomographic section, passing ~12 cm behind the glabella. (D) perfusion in set of horizontal sections.

conventional gamma-camera images. Horizontal tomographic sections (Fig. 1C) showed a rounded area of absent perfusion in the frontal lobe. The hyperactivity seen in the lateral two-dimensional image is in the adjacent gray matter of the frontal lobe, probably reflecting luxury perfusion. Hyperactivity is particularly evident behind the hematoma. Thus, unlike the two-dimensional images, the tomographic sections allow an exact definition of the extension and location of the functional impairment, avoiding artifacts due to superimposition of different brain structures.

Case 2. This patient presented with reversible ischemic attack from occlusion of the right internal cerebral artery (ICA). A left carotid angiogram (Fig. 2A) visualized both the anterior cerebral arteries but only the first centimeter of the right middle cerebral artery (MCA). Infusion of Kr-81m into the *left* ICA was performed. The conventional projections showed a normal uniform distribution in the left lateral view, slight presence of activity on the right side being detectable on both the anterior and the posterior views (Fig. 2B). Emission tomography allowed a more accurate definition of the perfusion patterns within the left hemisphere, as well as the left-to-right collateral circulation pathways. Coronal section 9 showed the collateral flow to the right MCA via the circle of Willis (Fig. 2C). Horizontal sections (Fig. 2D) showed the presence of separate patterns of collateral flow through both the right MCA and ACA.

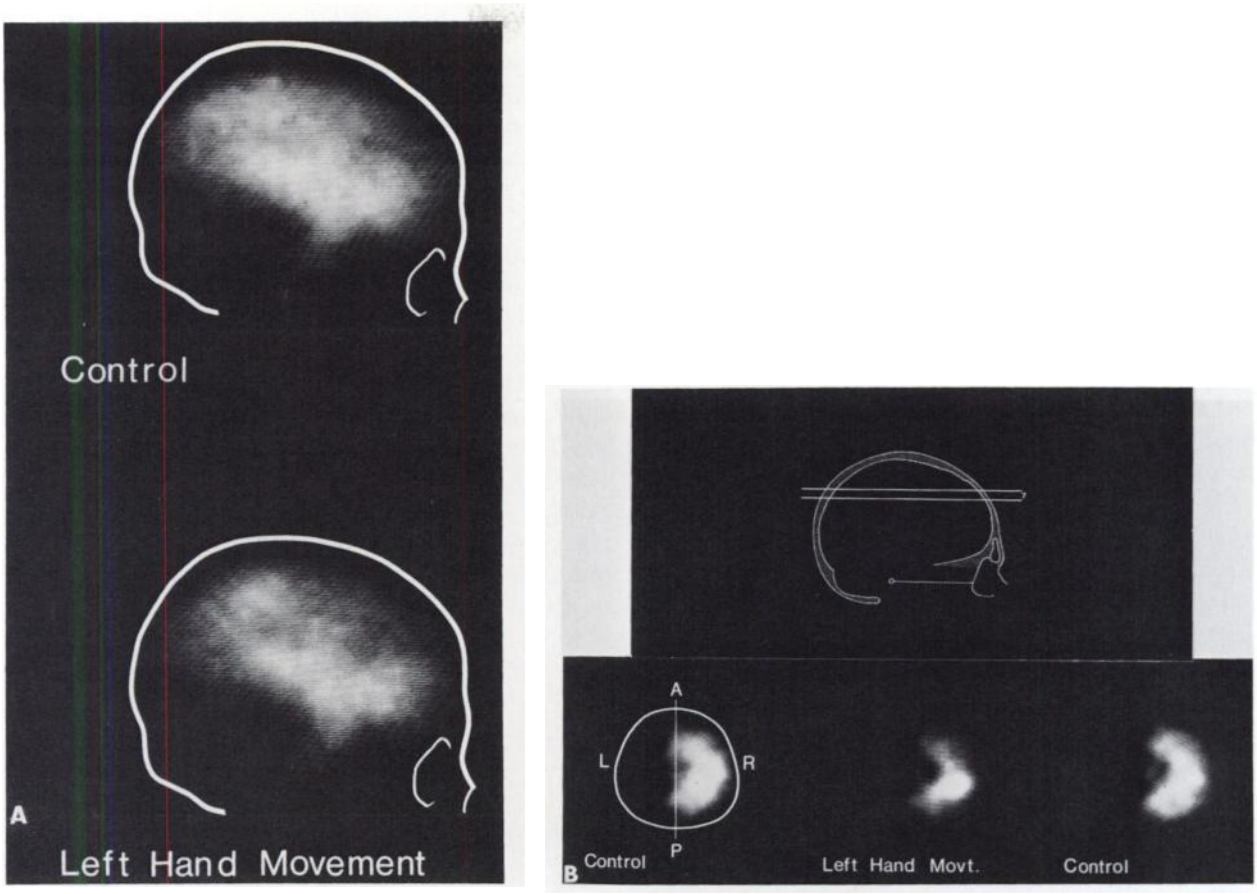

FIG. 3. Motor activation study of right hemisphere (clenching of left hand) (A) conventional perfusion views during right carotid infusion of Kr-81m (B) tomographic assessment of perfusion, showing relative flow increase to motor area for hand.

They also allow assessment of the relative distribution of the brain blood flow to different brain structures. Section 3 demonstrates that the watershed area, angiographically described between ACA and MCA distribution territory, corresponds to an area in which blood flow is effectively reduced; sections 4, 5, and 6 show the capability of the technique in resolving brain structures, such as the basal ganglia (thalamus, nucleus lentiformis). Higher sections (section 6) show greater perfusion to central and cortical gray matter relative to the white matter, which showed little activity.

Activation studies. Motor activation studies were carried out by asking the patient to conceive and to clench the hand contralateral to the studied hemisphere. Figure 3 shows the results of such an activation study. This patient has a small glioma in the white matter of the right frontal lobe; during right carotid infusion it could be seen in the right lateral view as an area of reduced perfusion (Fig. 3A, top). This was confirmed on low horizontal sections, while perfusion to higher sections (such as section 7, which passes through the Rolandic cerebral cortex) was normal (Fig. 3B, left). Left-hand clenching induced small changes of perfusion in the right lateral two-dimensional view (Fig. 3A, bottom), whereas tomography showed a marked increase of flow to the motor area for the hand relative to other brain structures (Fig. 3B, middle).

DISCUSSION

This study shows the feasibility of obtaining both horizontal and coronal tomographic reconstructions of the hemispheric distribution of cerebral perfusion using a single-photon emitter and a commercial rotating gamma camera. Tomographic reconstructions are particularly important for the functional assessment of a complex organ, such as the brain, where conventional views tend to show a uniform distribution of activity, due to superimposition of information from above and below the plane of interest. In the assessment of cerebral perfusion, tomographic reconstructions showed the following advantages over conventional two-dimensional views: (a) visualization of blood-flow distribution within brain structures (gray and white matter, basal ganglia); (b) more accurate location and evaluation of perfusion alterations; (c) better definition and evaluation of patterns of collateral circulation; and (d) greater sensitivity and specificity in detecting and describing blood-flow changes during physiological activation studies.

Regional cerebral perfusion was assessed by contin-

uous carotid infusion of Kr-81m. Under steady-state conditions, this method produces a flow image that contains the high counting rates required for high-resolution emission tomography. The other advantage of the Kr-81m technique, apart from the low radiation dose, is its capability of assessing rapid sequential changes of function, such as those induced by physiological or pharmacological activation of brain structures (Fig. 3).

On the other hand, the Kr-81m technique has a number of disadvantages. First of all, it provides images of hemispheric rather than of overall cerebral perfusion. In order to assess regional distribution of flow to the whole brain (rather than to the territory of the infused carotid artery), the tracer could be infused at the outflow of the left heart, or in the ascending aorta. However, this presupposes appropriate mixing of the tracer with arterial blood, which is probably an unwarranted assumption, since arterial blood enters the ascending aorta with inhomogeneous streaming patterns. Another shortcoming of the Kr-81m technique is that, at present, it merely provides a qualitative assessment of flow distribution rather than absolute flow values. Theoretically, the technique could be made quantitative; this would entail: (a) measuring the input concentration of Kr-81m and subsequently solving the Kr-81m equation (*14*) in a way similar to that recently developed for $C^{15}O_2$ brain blood-flow studies (T. Jones, personal communication); and (b) applying appropriate corrections to make the reconstructed slices truly quantitative. In particular, the correction for photon attenuation still needs to be optimized. In this study we used a correction algorithm that assumes uniform absorption within the head. However, recent studies comparing different methods of attenuation correction indicate that this assumption is probably not warranted (*15, 16*). In the future, transmission data should be more extensively used for attenuation correction in both positron and single-photon emission tomography.

No doubt the major, practical shortcoming of the Kr-81m technique is its invasiveness. This will probably limit its adoption for clinical measurements of cerebral blood flow, despite efforts to make the method quantitative and to substitute femoral or brachial catheterization for carotid puncture.

Nevertheless, in our hands this technique showed the feasibility of obtaining a tomographic assessment of regional cerebral blood flow using single-photon emitters and a commercial rotating gamma camera. Rotating cameras capable of providing horizontal and coronal reconstructions are now being produced by an increasing number of manufacturers, and in the near future their price will probably be only slightly in excess of that of a nonrotating camera with dedicated computer. In order to obtain emission tomography, however, rotating gamma cameras probably will need to be associated with steady-state methods. Special-purpose tomographic devices are now being designed and built in order to obtain single-photon *dynamic* emission tomography (*4*). On the other hand, progress in radiopharmaceutical science has recently made it possible to estimate cerebral function with steady-state methods, namely single intravenous injection of compounds extracted by the brain and labeled with positron emitters such as C-11 or F-18 (*17*). These steady-state methods are now being used, in association with specially built tomographs, for the noninvasive, three-dimensional assessment of brain blood flow and metabolism. The labelling of tracers for cerebral function with single-photon emitters such as Tc-99m or I-123—or at least the production of radiopharmaceuticals, so labeled, that could cross the blood-brain barrier—seems a not too distant goal, considering the rapid progress of radiopharmaceutical science (*18*). This combination of new advances in radiochemistry with single-photon emission computed tomography may result in accessible methods for assessing, noninvasively and in three dimensions, the behavior of cerebral function in man.

FOOTNOTES

*Selo, Milano, Italy.
†Simis 3, Informatek, U.S.A./France.

ACKNOWLEDGMENTS

We thank Professor L. Donato for support and M. M. Barr for technical help. We also thank colleagues of the M.R.C. Cyclotron Unit, Hammersmith Hospital, London, for active cooperation, and Mrs. H. Creed for secretarial help. The work was supported in part by the National Research Council of Italy (Progetto Finalizzato Tecnologie Biomediche) and by International Euratom Contract No. 228-76-7 BIO I/U.K. (Pisa-London).

APPENDIX

Compensation for tissue absorption. The present algorithm, used for attenuation correction, rests on the assumption that absorption of gamma photons within the absorbing medium is uniform. Thus, an analytical correction of attenuation artifacts can be obtained if the attenuation per unit length throughout the object, α, is considered constant.

When a gamma emitter is surrounded by a uniform absorbing medium, a projection, p, taken at an angle ϕ can be defined as:

$$p(r,\phi,\alpha) = \int_{-\infty}^{\infty} f(\rho,\Theta)\exp(-\alpha(D+1))dl.$$

where ρ and Θ are polar coordinates, $l = \rho\sin(\Theta-\phi)$, and D the distance between the center of the object and the detector plane.

Due to the air gap between body and collimators, the measured projections $p'(r,\phi,\alpha)$ must be corrected for attenuation in air between collimator and body contour,

$$p(r,\phi,\alpha) = p'(r,\phi,\alpha)\exp(-\alpha D(r,\phi)) \quad (1)$$

where $D(r,\phi)$ is the distance between collimator and body contour. This requires determination of body contour. If this is concave the procedure cannot be applied and a water bag must be added.

Reconstruction from attenuated projections. Let us write Eq. 1 as:

$$p(r,\phi,\alpha) = \int_{-\infty}^{\infty} f(\rho,\Theta)\exp(-\alpha\rho\sin(\theta-\phi))dl$$

and let us consider its Fourier transform:

$$P(R,\phi,\alpha) = \int_{-\infty}^{\infty}\int_{-\infty}^{\infty} f(\rho,\Theta)\exp(-\alpha\rho\sin(\Theta-\phi))\exp(-jrR)drdl.$$

This double integral can be written in polar coordinates as:

$$P(R,\phi,\alpha) = \int_{0}^{2\pi}\int_{0}^{\infty} f(\rho,\Theta)\exp(-\alpha\rho\sin(\Theta-\phi) - jR\rho\cos(\Theta-\phi))\rho d\rho\, d\Theta.$$

The problem is to find $F(R,\phi) = P(R,\phi,0)$ from $P(R,\phi,\alpha)$. It can be verified that the function of the three variables $P(R,\phi,\alpha)$ satisfies the partial derivative equation

$$\frac{\delta P}{\delta\alpha} = \frac{\alpha\delta P}{R\delta R} - \frac{j}{R}\frac{\delta P}{\delta\phi}$$

Solving this equation and setting the appropriate boundary conditions, the formula can be derived:

$$P(R,\phi,0) = P\left(\sqrt{R^2+\alpha^2}, \phi + jSh^{-1}\frac{\alpha}{R}, \alpha\right).$$

The evaluation of $P(R,\phi,\alpha)$ at radial frequencies $\sqrt{R^2+\alpha^2}$ can be obtained by interpolation. The calculation of the same function for complex values of ϕ is obtained by angular convolutions. The details of the algorithm are described in Ref. *13*.

In practice, a reconstruction is first performed using the attenuated projections, in order to acquire information on the body's contour. Then the correction algorithm is applied. This is shown more in detail in Ref. *13*.

REFERENCES

1. PHELPS ME: Emission computed tomography. *Semin Nucl Med* 7: 337-365, 1977
2. KUHL DE, EDWARDS RQ, RICCI AR, et al: The Mark IV system for radionuclide computed tomography of the brain. *Radiology* 121: 405-413, 1976
3. JARRITT PH, ELL PJ, MYERS MJ, et al: A new transverse-section brain imager for single-gamma emitters. *J Nucl Med* 20: 319-327, 1979
4. STOKELY EM, SVEINSDOTTIR E, LASSEN NA, et al: A single photon dynamic computer assisted tomograph (DCAT) for imaging brain function in multiple cross sections. *J Comput Assist Tomog* 4: 230-240, 1980
5. BUDINGER TF, GULLBERG GT: Three-dimensional reconstruction in nuclear medicine emission imaging. *IEEE Trans Nucl Sci* 21: 2-20, 1974
6. KEYES JW JR, ORLANDEA N, HEETDERKS WJ, et al: The humongotron—A scintillation camera transaxial tomograph. *J Nucl Med* 18: 381-387, 1977
7. MURPHY PM, THOMPSON WL, MOORE ML, et al: Radionuclide computed tomography of the body using routine radiopharmaceuticals. 1. System characterization. *J Nucl Med* 20: 102-107, 1979
8. FAZIO F, NARDINI M, FIESCHI C, et al: Assessment of regional cerebral blood flow by continuous carotid infusion of krypton 81m. *J Nucl Med* 18: 962-966, 1977
9. CLARK JC, HORLOCK PL, WATSON IA: Krypton-81m generators. *Radiochem Radioanal Lett* 25: 245-254, 1976
10. KAPLAN E, MAYRON LW: Evaluation of perfusion with the ^{81}Rb-^{81m}Kr generator. *Semin Nucl Med* 6: 163-192, 1976
11. KAY DB: The reconstruction of three-dimensional radionuclide sources by digital and optical processing. Doctoral Dissertation, University of Rochester, New York, 1976
12. BELLINI S, PIACENTINI M, CAFFORIO C, et al: Design of a computerized emission tomographic system. *Signal Processing* 1: 125-131, 1979
13. BELLINI S, CAFFORIO C, PIACENTINI M, et al: Compensation of tissue absorption in emission tomography. *IEEE Trans ASSP* 27: 213-218, 1979
14. FAZIO F, JONES T: Assessment of regional ventilation by continuous inhalation of radioactive krypton-81m. *Br Med J* 3: 673-676, 1975
15. BUDINGER TF, DERENZO SE, GULLBERG GT, et al: Emission computer assisted tomography with single-photon and positron annihilation photon emitters. *J Comput Assist Tomog* 1: 131-145, 1977
16. HUANG SC, HOFFMAN EJ, PHELPS ME, et al: Quantitation in positron emission computed tomography. 2. Effects of inaccurate attenuation correction. *J Comput Assist Tomog* 3: 804-814, 1979
17. REIVICH M, KUHL D, WOLF A, et al: The [^{18}F]fluorodeoxyglucose method for the measurement of local cerebral glucose utilization in man. *Circ Res* 44: 127-137, 1979
18. LOBERG MD, CORDER EH, FIELDS AT, et al: Membrane transport of Tc-99m-labelled radiopharmaceuticals. 1. Brain uptake by passive transport. *J Nucl Med* 20: 1181-1188, 1979